Evidence of nematic, hexagonal and rectangular columnar phases in thermotropic ionic liquid crystals

by FRANCK ARTZNER, MICHELE VEBER*, MARIANNE CLERC
and ANNE-MARIE LEVELUT

Laboratoire de Physique des Solides, bât.510, Université Paris Sud,
F-91405 Orsay Cedex, France

Dithiolium salts, with amphipathic character, are compounds of choice for investigations of the influence of an ionic feature upon mesomorphic properties. In this way, salts bearing a branched chain have been studied by SAXS. In spite of their rod-like shape, they exhibit only columnar mesophases, the supramolecular organization of which is close to that of cylindrical inverted micelles. Moreover, the nematic columnar phase, characterized by the loss of lateral positional correlations of the columns themselves, is one of the first examples of such behaviour in the case of thermotropic liquid crystals.

1. Introduction

The role of specific intermolecular interactions, such as hydrogen bonding [1, 2], charge transfer [3, 4] and coulombic forces, in the formation or stabilization of liquid crystalline phases has only recently been appreciated. Long-range and strong ionic interactions have been thoroughly studied in the case of lyotropic systems [5] and anhydrous soaps [6]. Moreover, the few known examples of thermotropic ionic liquid crystals [7–10] show that the ionic feature has a strong influence upon the mesomorphic properties. Besides, recent developments of metallomesogens [11] have caused a new interest in the topic of thermotropic ionic liquid crystals.

In such an area, we have been interested for a long time in the synthesis and study of 3,5-diaryl-1,2-dithiolium salts [8, 9] and 2,4,6-triarylpyrylium salts [10]. In the latter case, for the salts with very short alkoxy chains (ethoxy and propoxy), the high temperature motion of the anions has been shown to be responsible for the appearance of a columnar hexagonal phase D_h. In the case of dithiolium salts, columnar hexagonal phases can be obtained with four paraffinic chains [8], and lamellar SmA phases with two or three chains [9]. Also in this case, it seems that the ionic feature of the salts plays an important role, since some neutral compounds with the same 'banana' shape [12] (e.g. isoxazole or pyrazole derivatives [13]) exhibit only lamellar and no columnar mesophases. Thus, dithiolium salts are molecules of choice for investigating the influence of ionic features upon liquid crystalline properties.

Until now, only linear chains have been grafted to the heteroaromatic, ionic, rigid core of the dithiolium cation. The aim of this work was to study the influence of a ramified (branched) chain upon the mesomorphic properties. Racemic mixtures of the salts **1** were synthesized and their mesomorphic properties investigated by optical microscopy and DSC. In addition, X-ray diffraction experiments with conventional equipment and using synchrotron radiation were performed on the salt **1a** ($n = 12$ in scheme 1), in order to establish fully the nature of the mesophases. In spite of the rod-like shape of the molecules, all the liquid crystalline phases are columnar, with a supramolecular organization similar to that of amphiphilic molecules. The columns can be stacked in either rectangular or hexagonal 2D lattices or without lateral positional correlations, in a nematic columnar phase, N_{col}, which has been observed only a few times in the case of thermotropic liquid crystals [2, 4].

2. Synthesis

Racemic mixtures of dithiolium salts **1a–d** were synthesized according to scheme 1, by heterocyclization of chalcones **4a–d** in an acidic medium. The chalcones were obtained by condensation of 3,4-dialkoxyacetophenones **3a–d** [8] and the 4-alkoxybenzaldehyde **2** in the presence of a catalytic amount of sodium hydroxide. The benzaldehyde **2**, bearing a 2-octyloxy chain, was synthesized by a Mitsunobu reaction between 4-hydroxybenzaldehyde and octan-2-ol [14].

3. Optical microscopy and DSC

The mesomorphic properties of salt **1a** ($n = 12$) were investigated by Differential Scanning Calorimetry using

*Author for correspondence.
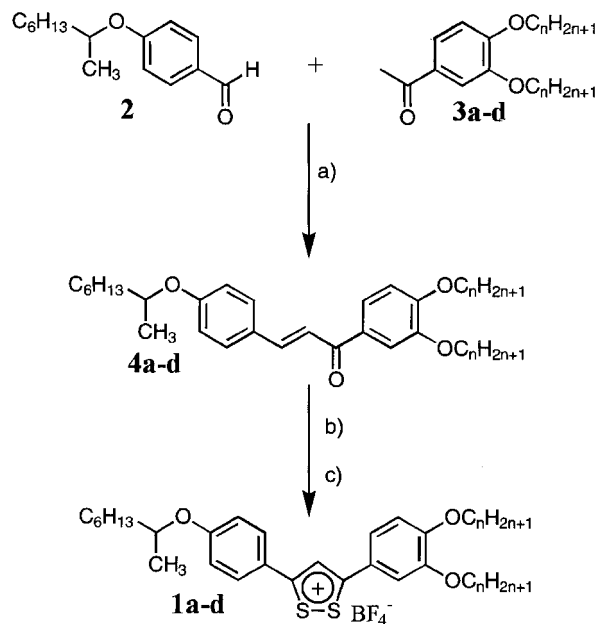
Scheme 1. (a) NaOH (cat), EtOH, 50°C, 12 h, (b) P_4S_{10}, 150°C, 30 min, (c) HBF$_4$, AcOH, 120°C, 1 h. For **1a–d**, see the table.

a DSC-7 apparatus operated at 5°C min^{-1} under nitrogen and by microscopic observations using a Leitz orthoplan polarizing microscope equipped with a Mettler FP52 hot stage and an FP5 central processor. DSC (figure 1) established that salt **1a** exhibits, upon heating, a double melting behaviour (113 and 151°C) to give a stable mesophase (called X). By slow cooling of the mesophase X, two low enthalpic transitions are detected at 148°C and 115°C, which are attributed to mesophase–mesophase transitions (X to Y at 148°C, and
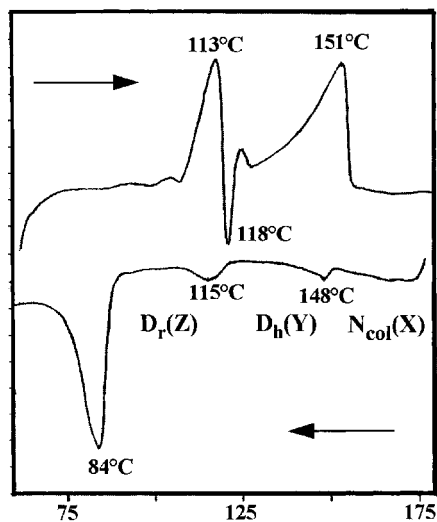

Figure 1. DSC thermogram of the salt **1a** (5°C min^{-1}): ($\rightarrow$) heating, ($\leftarrow$) cooling.

Y to Z at 115°C). Further cooling leads to crystallization at 84°C. No clearing transition is detected by DSC.

Observations by polarizing optical microscopy gave further results: upon cooling the isotropic phase of **1a**, formation of bâtonnets in homeotropic areas (phase X in figure 2(a)) occurs between 176–173°C. These bâtonnets then coalesce to a fan-shaped texture at 148°C (phase Y in figure 2(b)), characteristic of hexagonal mesophases. At 115°C, the smooth fan-shapes become wrinkled (phase Z in figure 2(c)).

4. X-ray diffraction and SAXS
4.1. *Studies of aligned samples*

An aligned sample of salt **1a** was studied by X-ray diffraction with an experimental set-up described elsewhere [9] using a point-focused monochromatic X-ray beam ($\lambda CuK_\alpha = 1\cdot541$ Å), where the sample, in a capillary tube (1 mm) is placed in a magnetic field (1·7 T). The mesophase X could be aligned at 170°C under the influence of the magnetic field. At 155°C, the observed pattern exhibits a diffuse ring at wide angles ($s = 1/4\cdot5$ Å^{-1}) corresponding to the molten parts of the molecules. In addition, two rather sharp symmetric peaks ($s = 1/39\cdot5 \pm 0\cdot5$ Å^{-1}), stronger along the magnetic field direction, are observed at small angles. No higher orders of reflection are detected. On further cooling, only the small angle pattern changes: at 140°C (phase Y in figure 3) three peaks, still aligned along the magnetic field direction, are observed in a $1:3^2:2$ ratio characteristic of a hexagonal lattice ($a = 44\cdot5 \pm 0\cdot5$ Å). The X-ray pattern at 105°C (phase Z) seems to correspond to a hexagonal phase ($a = 46\cdot7 \pm 0\cdot5$ Å) with weak core–core interactions ($s = 1/3\cdot6$ Å^{-1}) along the column axis as shown by a diffuse scattering perpendicular to the magnetic field.

4.2. *The hexagonal and rectangular mesophases*

In order fully to identify the mesophases of **1a**, a Small Angle X-ray Scattering study was carried out on the synchrotron beam line D43 at the LURE laboratory using a point-focused monochromatic X-ray beam ($\lambda = 1\cdot45$ Å) having low divergence $\Delta q = 2\cdot5 \times 10^{-3}$ Å^{-1}. Quantitative data at fixed temperature were obtained with image plates as detector, and varying temperature data with a CCD camera. In the latter case, the acquisition time of each profile was shorter than 10 seconds. The phase Y was confirmed to be a columnar hexagonal D_h phase (Col$_h$) ($a = 43\cdot1$ Å) by the observation at 145°C of three peaks corresponding to a 2D hexagonal lattice (**1 0 0**: $d_{exp} = 37\cdot37$ Å, $d_{th} = 37\cdot35$ Å; **1 1 0**: $d_{exp} = 21\cdot58$ Å, $d_{th} = 21\cdot56$ Å; **2 0 0**: $d_{exp} = 18\cdot65$ Å, $d_{th} = 18\cdot67$ Å). At 95°C, the mesophase Z is a columnar rectangular D_r phase (Col$_r$), close to a hexagonal phase, as shown by the doubled peaks in the small angle area (figure 4). These
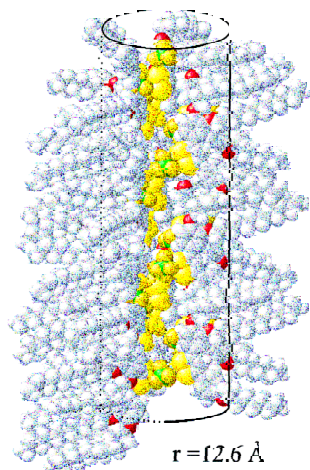
Scheme 2. Schematic organization of salts **1** inside the columns of the hexagonal D_h mesophase.

peaks were indexed as 1 1 0 (**B**: $d = 39\cdot4$ Å) and 2 0 0 (**A**: $d = 42\cdot1$ Å), so that their intensities are in agreement with their multiplicity factors (i.e. 4 and 2, respectively). Reflections 1 0 0 and 0 1 0 are not observed. Because the reflection 2 1 0 ($d = 30\cdot6$ Å) is not detected, centred space groups C were preferred to primitive ones. The highest symmetry 3D space group $C_{2/m2/m2/m}$ corresponding to the 2D plane group Cmm ($a = 44\cdot6 \pm 0\cdot1$ Å, $b = 84\cdot2 \pm 0\cdot2$ Å) is proposed.

### 4.3. *Supramolecular organization inside the columns*

The supramolecular organization inside the columns is quite different from that usually observed in columnar phases of disc shaped molecules, since the shape of the molecules is more banana-like than discotic. Evaluating the density of the linear chain salts along the columns ($1/d_{core}$) could give a first insight into this organization in the hexagonal phase: $1/d_{core} = 3^{\frac{1}{2}}/2(\rho N_A / M_W)a^2$, where a is the hexagonal lattice parameter, M_W is the molecular mass of the salt **1a** (838), N_A is the Avogadro Number and ρ is the density. In the case that the density ρ is close to 1 (which is true for the columnar phases of dithiolium salts [8]), $1/d_{core} = 1\cdot16$ Å^{-1}. A characteristic length along the columns is the observed distance of $3\cdot6$ Å, which corresponds approximately to the distance between molecular cores. This value of d_{core} means that there are approximately four salts in a slice of a column with a thickness of $3\cdot6$ Å; this is large compared with other values [8, 15, 16]. A second insight into the supramolecular arrangement could be given by evaluation of the radial profile of electronic density of the columns in the hexagonal phase: such different profiles have been obtained in order to compare theoretical intensities of the diffraction peaks with the experimental values, corrected for the Lorentz-polarization factor ($I_{100} = 1000$,
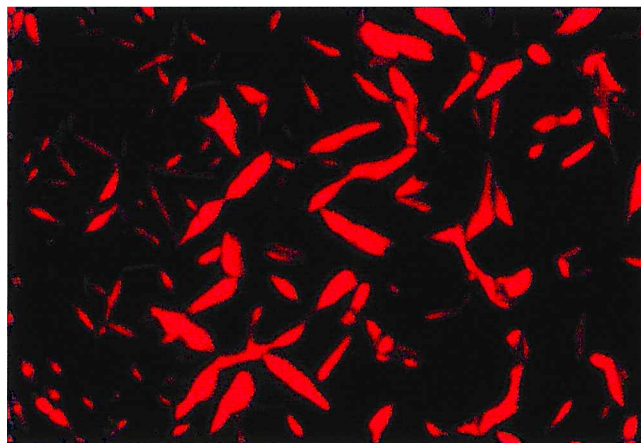
(*a*)

(*b*)
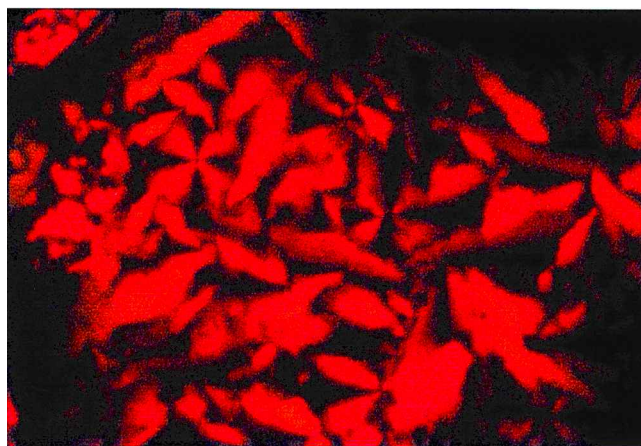
(*c*)

Figure 2. Photomicrographs of salt **1a**: (*a*) at 155°C N_{col}, (*b*) at 147°C D_h and (*c*) at 115°C D_r, viewed between crossed polarizers.
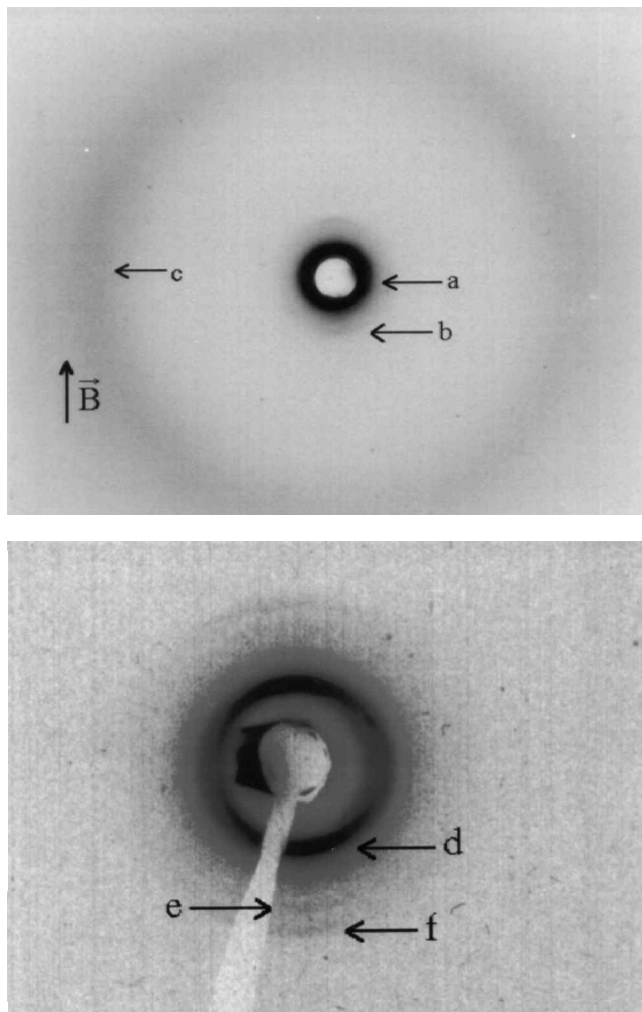
Figure 3. X-ray diffraction pattern of salt **1a** in the D_h phase at 140°C after cooling in the magnetic field (1·7 T). Top: **a** and **b**, $s = 1/38·5\,\text{Å}^{-1}$ and $s = 1/19·3\,\text{Å}^{-1}$, respectively; **c**, $s = 1/4·5\,\text{Å}^{-1}$. Bottom: magnification of the small angles region; **d**, **e** and **f**, $s = 1/38·5$, $1/22·2$ and $1/19·3\,\text{Å}^{-1}$, respectively.

$I_{110} = 3$, $I_{200} = 8$). The best result was obtained with a simple model [10] of the profile which corresponds to two parts with different electronic densities separated by a sharp cylindrical interface; the former part is inside a column of radius 12·6 Å and the latter part surrounds the column. If we assume that the cores are inside the columns, we now have access to the volume of the core $V_{core} = d_{core}\pi(r_{core})^2 = 430\,\text{Å}^3$, the volume per methylene group $V_{CH_2} = (M_W/\rho N_A - V_{core})/32 = 30\,\text{Å}^3$, and the surface area per aliphatic chain at the interface between the aromatic and aliphatic parts (i.e. the surface of the cylinder) $S_{CH_2} = 2\pi r_{core}d_{core}/3 = 23\,\text{Å}^2$. V_{core} is in agreement with the measured volume from a CPK model; V_{CH_2} and S_{CH_2} are normal for this type of mesophase [8, 15, 16]. These agreements confirm that the cores are

inside the cylinder. Thus, the supramolecular organization of the molecules inside the columns is driven by the amphipathic feature of the salts. They are arranged into long cylindrical aggregates: i.e. heads of amphiphiles (heteroaromatic cores and anions) inside the columns, surrounded by aliphatic chains without any positional order along the column axis (scheme 2).

The last point to discuss concerning the hexagonal phase is the increase of the lattice parameter on decreasing the temperature, as indicated by the decrease of q_{100} upon cooling D_h (figure 4). The thermal expansion coefficient can be evaluated: $a^{-1}\Delta a/(\Delta T) = -2·0 \times 10^{-3}\,\text{K}^{-1}$. Similar negative coefficients have previously been observed for disordered D_h phases [17]. This effect most likely reflects the increase in the chain disorder on increasing the temperature. At low temperature, the ratio of methylene groups which are in the *all-trans* conformation is larger, resulting in larger lengths of extended aliphatic chains, while the chain disorder introduced upon heating results in shorter lengths of extended aliphatic chains.

4.4. *The nematic columnar phase*

The birefringent high temperature phase X exhibits a broad peak in the small angle area ($s = 1/36·3\,\text{Å}^{-1}$ at 153°C in figure 5), showing short range positional order with a mean distance between scattering objects of 36·3 Å. This distance is close to the mean distance between columns in the hexagonal phase, 37·4 Å, and longer than the molecular length (34 Å by CPK models). Thus, the scattering objects are not molecules, but could be small or large aggregates of molecules which exhibit long range orientational order. Because both phases at lower temperature are columnar in nature, and the orientation of the aligned samples is preserved through the transition, we can suppose that the phase X is columnar in nature too. This hypothesis is supported by the following facts: (i) shearing aligns the phase temporally, which is characteristic of long and anisotropic objects, such as polymers or columns; (ii) the peak's profile fits to a Lorentzian curve superimposed over a linear background (figure 5); and (iii) the correlation length ζ deduced from the fit is close to 60 Å. Such behaviour has been observed in the case of nematic columnar phases of diamides [2] or of copper soaps [18], and the peak profile was attributed to the spatial extension of some columnar order. Therefore, the phase X is a nematic columnar N_{col} phase where, for example, the molecules are stacked in columns which possess no long range lateral positional order. Consequently, the D_h to N_{col} transition could be interpreted as the melting of the 2D hexagonal lattice, without complete destruction of the columns.
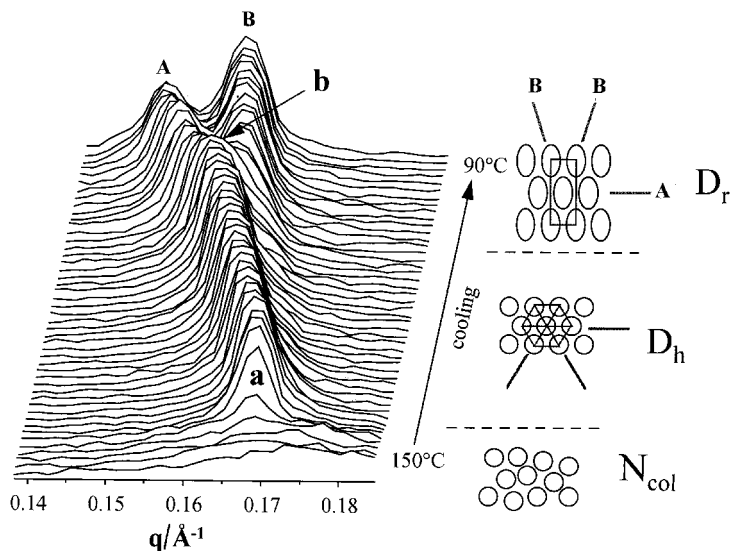
Figure 4. SAXS experiments on **1a**: intensities of the profile upon cooling ($10°C \, min^{-1}$) and the corresponding 2D space groups (right). **a** and **b** correspond to the N_{col} to D_h and D_h to D_r transitions, respectively. **A** and **B** are indexed as the 2 0 0 and 1 1 0 reflections; directions of reticular planes are indicated.
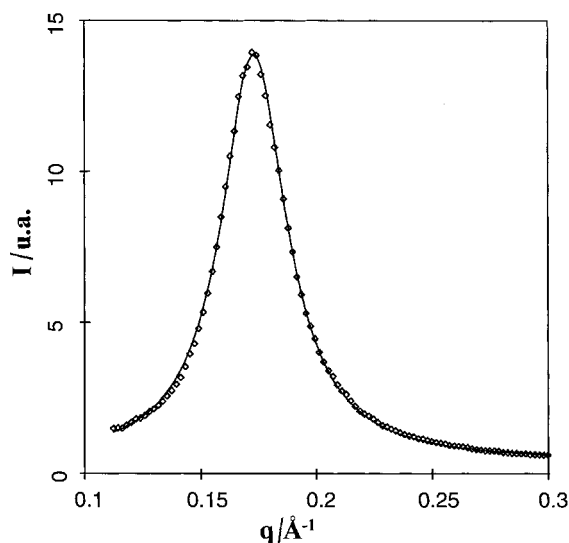

Figure 5. SAXS experiments on **1a**: intensity of the profile of N_{col} obtained at 153°C. The experimental peak (open diamonds) and the fit by a Lorentzian curve superimposed over a linear background (—).

4.5. *The phase sequence*

We have shown that, depending on the temperature, salt **1a** exhibits three different columnar mesophases D_r, D_h and N_{col} (scheme 3). The phase sequence (see the table) was totally elucidated by recording radial small angle profiles (SAXS) at different temperatures. Upon cooling the N_{col} phase, first the transition to a hexagonal lattice (**a** in figure 4), then to a rectangular lattice (**b** in figure 4) and finally crystallization to a metastable crystal C_{21} is observed. Heating leads to the melting of the crystal C_{21} forming the rectangular mesophase, which is close to a hexagonal one. Then, crystallization to the

stable crystal C_{22} occurs, which melts and transforms into N_{col}.

5. Influence of the linear chain length

The influence of the linear chain length was investigated by the studies of salts **1b–d** by polarizing microscopy and differential scanning calorimetry.

The results are summarized in the table: the four compounds exhibit the same phase sequence upon cooling, but the hexagonal mesophase is monotropic when n is even and enantiotropic when n is odd. The melting temperatures and temperatures of both mesophase–mesophase transitions show a small odd–even effect. This has only been observed a few times in the case of D_h [17].

6. Conclusion

Dithiolium salts with a ramified chain **1** exhibit a rich polymorphism independently of the length of the linear chains. Using different complementary experiments, two main results have been found. First, the driving force for the supramolecular organization is more the amphipathic feature of the salts than their shape: dithiolium salts form long columnar aggregates similar to long inverted cylindrical micelles. At low temperature, the columns could be arranged in D_h or D_r mesophases. Second, the higher temperature mesophase is nematic columnar; the columns are almost parallel without long range lateral positional correlations. To the best of our knowledge, this is the first time that a N_{col} phase has been observed in a thermotropic ionic liquid crystal material. This confirms the idea that some specific interactions are necessary to obtain nematic columnar mesophases, because in other quoted examples of N_{col}
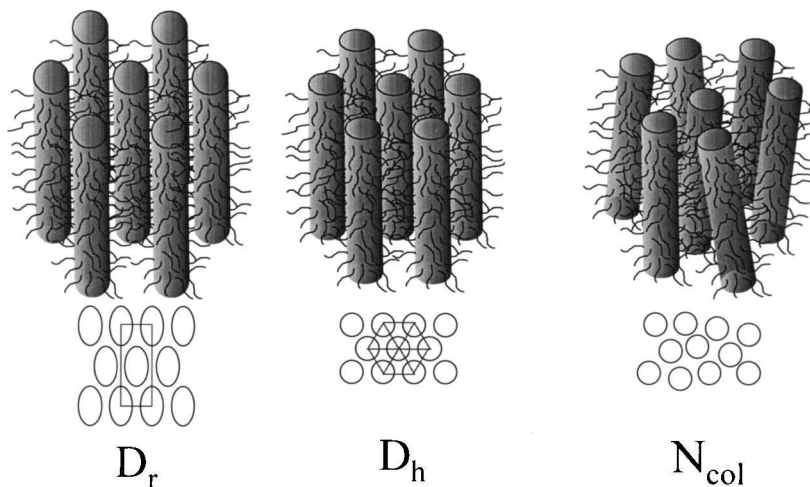
$$D_r \qquad D_h \qquad N_{col}$$

Scheme 3. Schematic representation of the organization of the columns of the salts **1**.

Table 1. Transition temperatures and transition enthalpies of the dithiolium salts

Salts	n	Transition temperatures/°C (transition enthalpies/kJ mol^{-1})
1a	12	$C_{r1} \underset{84(13)}{\overset{113}{\rightleftarrows}} D_r \xrightarrow{118} C_{r2} \overset{151(15)}{\rightleftarrows} N \overset{176a}{\rightleftarrows} I$; $\underset{115(1\cdot1)}{} D_h \underset{148(0\cdot8)}{} $
1b	11	$C_r \overset{139(8)}{\underset{115(10)}{\rightleftarrows}} D_r \xleftarrow{135(0\cdot4)} D_h \overset{154(0\cdot5)}{\rightleftarrows} N \overset{178a}{\rightleftarrows} I$
1c	10	$C_r \overset{145(24)}{\underset{107(14)}{\rightleftarrows}} D_r \xleftarrow{126(1\cdot1)} D_h \overset{144a}{\rightleftarrows} N \overset{174a}{\rightleftarrows} I$
1d	9	$C_r \overset{138(23)}{\underset{102(15)}{\rightleftarrows}} D_r \xleftarrow{132(1\cdot9)} D_h \overset{148(0\cdot9)}{\rightleftarrows} N \overset{172a}{\rightleftarrows} I$

[a] Enthalpy too small to be measured; transition temperature determined by optical microscopy.

either hydrogen bonding [2], or charge transfer [4] interactions stabilize the long columns. Such interactions are so strong that the 2D lattice can melt without complete destruction of the columns.

7. Experimental

7.1. *General*

Dithiolium salts **1** and chalcones **2** were prepared according to published procedures. ^{1}H NMR and ^{13}C NMR spectra were recorded on a Brucker AC300 spectrometer; CDCl$_3$ was the solvent, with TMS as reference. Results for one chalcone (**4a**) and one dithiolium salt (**1a**) are quoted below.

7.2. *Chalcone* **4a**

Yield 66%, m.p. 44°C. ^{1}H NMR [(CDCl$_3$), 300m Hz]: δ 0·85 (9H, t, $J = 6\cdot7$ Hz, CH$_2$–CH_3); 1·25 (3H, d, $J = 6\cdot1$ Hz, CH–CH_3); 1·17–1·72 (46H, m, CH_2); 1·72–1·84 (4H, m, O–CH$_2$–CH_2); 3·97–4·06 (4H, m, O–CH_2); 4·35 (1H, m, O–CH); 6·81–6·87 (3H, m, ArH); 7·36 (1H, d, $J = 15\cdot6$ Hz, C=CH); 7·49–7·59 (4H, m, ArH); 7·76 (1H, d, $J = 15\cdot6$ Hz, C=CH). ^{13}C NMR [(CDCl$_3$), 300 mHz]: δ 188·5 (s, C=O); 159·8, 153·5, 148·9, 131·3, 127·4 (s, C phenyl); 143·5, 129·9, 122·7, 119·2, 115·8, 113·1, 111·6, (d, CH phenyl and alkene); 74·0 (d, O–CH); 69·0, 69·2 (t, O–CH_2); 36·0, 31·7, 31·5, 29·3, 29·0, 25·9, 25·2, 22·5 (t, CH$_2$); 19·3, 14·0 (q, CH$_3$).

7.3. *Dithiolium salts* **1a**

Yield 13%. ^{1}H NMR [(CDCl$_3$), 300 mHz]: δ 0·85 (9H, t, $J=6·7$ Hz, CH$_2$–CH$_3$); 1·25 (3H, d, $J=6·1$ Hz, CH–CH$_3$); 1·17–1·72 (46H, m, CH$_2$); 1·72–1·84 (4H, m, O–CH$_2$–CH$_2$); 3·97–4·12 (4H, m, O–CH$_2$); 4·48 (1H, m, O–CH); 6·81 (1H, d, $J=9$ Hz, ArH); 6·98 (2H, d, $J=9$ Hz, ArH); 7·20 (1H, s, ArH); 7·67 (1H, d, $J=9$ Hz, ArH); 8·00 (2H, d, $J=9$ Hz, ArH); 8·79 (1H, s, H of dithiolium ring). MS: 751 (C$^{\oplus}$), 648 (C$^{\oplus}$–C$_8$H$_{17}$).

References

[1] PALEOS, C. M., and TSIOURVAS, D., 1995, *Angew. Chem.*, **107**, 1839; 1995, *Angew. Chem. Int. Ed. Engl.*, **34**, 1696.

[2] ALBOUY, P. A., GUILLON, D., HEINRICH, B., LEVELUT, A. M., and MALTHÊTE, J., 1995, *J. Phys. II France*, **5**, 1617.

[3] GIONIS, V., STRZELECKA, H., VEBER, M., KORMAN, R., and ZUPPIROLI, L., 1986, *Mol. Cryst. liq. Cryst.*, **137**, 365.

[4] PRAEFCKE, K., SINGER, D., KOHNE, B., EBERT, M., LIEBMANN, A., and WENDORFF, J. H., 1991, *Liq. Cryst.*, **10**, 147; BENGS, H., KARTHAUS, O., RIGSDORF, H., BAEHR, C., EBERT, M., and WENDORFF, J. H., 1991, *ibid.*, **10**, 161.

[5] ISRAELACHVILI, J., 1991, *Intermolecular & Surfaces Forces*, 2nd Edn. (London: Academic Press), p. 366.

[6] MIRNAYA, T. A., PRISYAZHNY, V. D., and SHCHERBAKOV, V. A., 1989, *Russ. chem. Rev.*, **58**, 821.

[7] BRUCE, D. W., DONIO, B., HUDSON, S. A., LEVELUT, A. M., MEGTERT, S., PETERMANN, D., and VEBER, M., 1995, *J. Phys. II France*, **5**, 289; ARKAS, M., YANNAKOPOULO, K., PALEOS, C. M., WEBER, P., and SKOULIOS, A., 1995, *Liq. Cryst.*, **18**, 563.

[8] STRZELECKA, H., JALLABERT, C., VEBER, M., DAVIDSON, P., LEVELUT, A. M., MALTHÊTE, J., SIGAUD, G., SKOULIOS, A., and WEBER, P., 1988, *Mol. Cryst. Liq. Cryst.*, **161**, 403; STRZELECKA, H., JALLABERT, C., and VEBER, M., 1988, *Ibid.*, **156**, 355.

[9] VEBER, M., JALLABERT, C., STRZELECKA, H., JULLIEN, O., and DAVIDSON, P., 1990, *Liq. Cryst.*, **8**, 775.

[10] VEBER, M., SOTTA, P., DAVIDSON, P., LEVELUT, A. M., JALLABERT, C., and STRZELECKA, H., 1990, *J. Phys. France*, **51**, 1283.

[11] NEVE, F., 1996, *Adv. Mater.*, **8**(4), 277.

[12] GRAMSBERGEN, E. F., and DE JEU, W. H., 1983, *Phys. Lett.*, **97A**(5), 199.

[13] BARBERA, J., CATIVIELA, C., SERRANO, J. L., and ZURBANO, M. M., 1992, *Liq. Cryst.*, **11**, 887.

[14] BAENA, M. J., BARBERA, J., ESPINET, P., EZCURRA, A., ROS, M. B., and SERRANO, J. L., 1994, *J. Am. chem. Soc.*, **116**, 1899.

[15] LEVELUT, A. M., MALTHÊTE, J., DESTRADE, C., and NGUYEN, H. T., 1987, *Liq. Cryst.*, **6**, 877.

[16] ZINSOU, A., VEBER, M., STRZELECKA, H., JALLABERT, C., and LEVELUT, A. M., 1994, *Liq. Cryst.*, **17**, 513.

[17] ZAMIR, S., SINGER, D., SPIELBERG, N., WACHTEL, E. J., ZIMMERMAN, H., POUPKO, R., and LUZ, Z., 1996, *Liq. Cryst.*, **21**, 39.

[18] SEGHROUCHNI, B., and SKOULIOS, A., 1995, *J. Phys. II France*, **5**, 1385.